Available online at www.sciencedirect.com

ScienceDirect

Energy Procedia 92 (2016) 515 – 522

Energy Procedia

6th International Conference on Silicon Photovoltaics, SiliconPV 2016

Simultaneous contacting and interconnection of passivated emitter and rear solar cells

Henning Schulte-Huxel[a,*], Jan-Hendrik Petermann[a,#], Susanne Blankemeyer[a], Verena Steckenreiter[a], Sarah Kajari-Schroeder[a], Rolf Brendel[a,b]

[a]*Institute for Solar Energy Research Hamelin (ISFH), Am Ohrberg 1, D-31860 Emmerthal, Germany*
[b]*Institut für Festkörperphysik, Leibniz Universität Hannover, Appelstraße 2, D-30167 Hannover, Germany*

Abstract

The back end process of passivated emitter and rear cells (PERC) consists of at least one laser process and three screen-printing steps followed by the stringing and tabbing of the cells. To reduce the number of steps we have developed a process that metallizes the rear side including contact formation and simultaneously interconnects the cells. We attach an Al foil to an encapsulant layer. By laser processing we form 'laser-fired and bonding contacts' (LFBC) on the passivated rear side of the solar cells. The Al foil contacting the rear is laser welded to the Ag screen-printed front side metallization of the next cell and thus forms the cell interconnection. The laser contacts on the rear show a surface recombination velocity S_{cont} for the contact regions of 1000^{+1000}_{-500} cm/s and a contact resistivity of 3.52 mΩcm². We present a first proof-of concept module combining the in-laminate Ag-Al laser welding and the LFBC reaching an efficiency of 18.4%. In accelerated aging test modules show no degradation (< 1% in efficiency) after 100 humidity-free cycles.

Peer review by the scientific conference committee of SiliconPV 2016 under responsibility of PSE AG.

Keywords: PERC solar cells; module interconnection; laser fiered contacts; laser welding

* Corresponding author. Tel.: +49-5151-999-303; fax: +49-5151-999-400.
E-mail address: h.schulte-huxel@isfh.de

[#] Now with iNOEX GmbH, Melle, Germany

Peer review by the scientific conference committee of SiliconPV 2016 under responsibility of PSE AG.
doi:10.1016/j.egypro.2016.07.135

1. Introduction

Recently screen-printed PERC solar cells have shown an increased efficiency up to 22.1% on 6” wafers [1]. To decrease cost per watt peak the increase of efficiency should be combined with the reduction of process complexity and steps. Combing the cell back-end processes and the cell interconnection simplifies the process flow. The PERC cells feature local contacts in the passivation layer on the rear that are formed by laser ablation. This process is termed laser contact opening (LCO) [2]. Additional to a screen printed Al layer that forms an Al back surface field (BSF) layer, Ag pads have to be applied in a second printing step. Laser fired contacts (LFC) [3] are an alternative to LCO and screen-printing. The LFC processes uses a laser to form the BSF from an evaporated or screen-printed Al layer or an Al foil [4]. Bitnar et al. indicated in a patent [5] that by applying additional metal structures on the Al foil an interconnection may be enabled. Independently of the Al-Si contact formation by LCOs or LFCs, the cells are interconnected at the end by soldering. Here, we present combined process for the metallization and interconnection of PERC cells. We use an Al foil attached to an ethylene-vinyl acetate (EVA) sheet to contact the rear side by ‘laser-fired and bonding contacts’ LFBCs [6,7] and also to interconnect the cells. Thereby, we avoid the stringing-tabbing process for cell interconnection, two screen-printing processes as well as the Ag consumption for the pads and require only one additional laser process for contacting the front side, where we laser weld the Al foil to the Ag front grid within the laminate.

2. Metallization and interconnection process

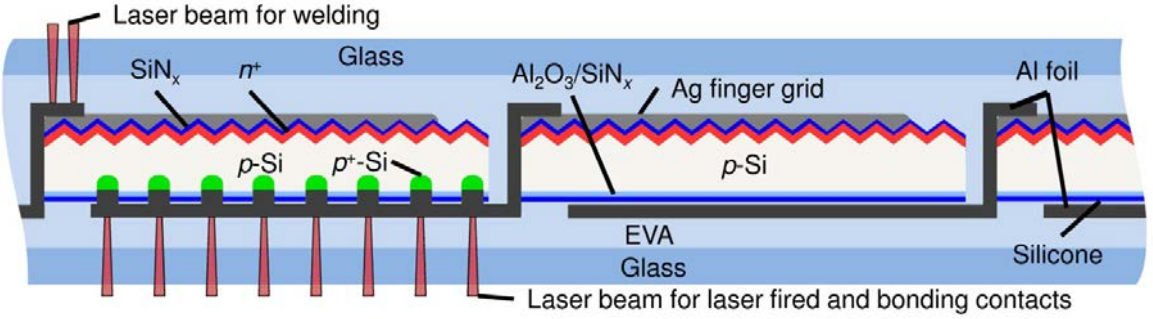

Fig. 1. Schematics of the LFBC used for cell rear side metallization and interconnection. An Al foil is attached to an EVA/glass substrate for mechanical support. Laser processing is done on the rear to form the LFBCs and on the front to weld the Al foil to the Ag metallization.

Fig.1 sketches the LFBC interconnection that we investigate in this paper. For contacting and interconnection the solar cell we use household Al-foil with a thickness of 13 µm. We laminate at 75°C the Al foil to an EVA sheet and a glass substrate for mechanical support. To enable a series interconnection, we structure the Al layer by a laser. The solar cells are processed as described in [8], however they are only metallized on the front side by Ag screen-printing. On their passivated rear side (AlO_x and SiN_x) we apply a thin layer of silicone (Tectosil, Wacker) in order to seal the space between the cells and the Al layer in the final module. We place the cells on the Al/EVA stack. The Al foil that contacts the rear side of one cell is in contact with the busbar of the next solar cell as shown in Fig.1. The cells are laminated with an EVA layer and a glass on the front side, which presses all components onto each other. We perform the LFBC process on the rear. On the front side we perform laser welding within the laminate to contact the Al foil to the Ag screen printing. For external connection we laser weld Al-clad copper connectors to the Al foil, see also Fig. 5. For all laser processes we use a Nd:YAG fiber laser (IPG YLP-c2-1500-15-30) which emits laser pulses with a duration of 1.3 µs at 1064 nm.

3. Results

3.1. Rear contact recombination

In order to determine the surface recombination velocity S_{cont} of the laser contacts we use floatzone *p*-type Si (resistivity ρ = 1.5 Ωcm; thickness w = 280 µm). We passivate the wafers on both sides with a stack of AlO_x (20nm) and SiN_x (100 nm). They are contacted by LFBCs to the Al-foil using line contacts with a pitch P between 250 µm and 2500 µm. The width b of the molten Al foil after laser processing is 83 µm as determined by an optical microscope through the glass substrate, which we assume to be the width of the contact lines [7]. However, the effective contact width between Al and Si, where the contact is formed through the dielectric layer, might be smaller.

We determine the effective charge carrier lifetime τ_{eff} by infrared lifetime mapping [9], see inset in Fig. 2. Squares with different pulse energies and line pattern are visible. In the region marked by the dashed square we determine the surface recombination velocity of the passivated area S_{pass} to be 3.5 cm/s under the assumption of bulk lifetime τ_b is limited by Auger recombination [10]. In region marked by the dashed rectangle we use pulse energies of 1.2 mJ and vary the pitch P between the lines from 0.25 mm to 2.5 mm. Fig. 2 shows the measured effective surface recombination velocity S_r of the laser treated area in dependence on the pitch P. We use the Fischer-model [11] to determine the surface recombination velocity S_{cont} for the laser contacted regions to be 1000^{+1000}_{-500}cm/s.

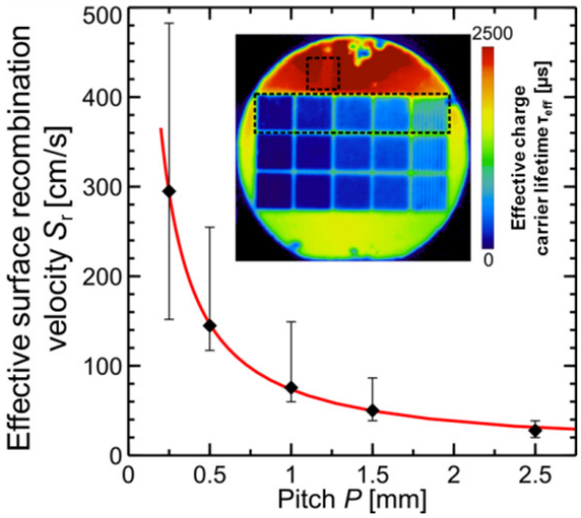

Fig. 2. Calculated effective surface recombination velocity S_r in dependence on the pitch P (black symbols. The red line is the fit according the Fischer-model. The inset shows the ILM measurements and the dashed boxes the areas used to determine S_{pass} and S_{cont}.

3.2. Rear contact series resistance

The series resistance has a critical impact on the module performance. We use *p*-type Si wafer (ρ = 0.5 Ωcm; w = 200 µm), which we passivate one side with AlO_x and SiN_x. The other side features a diffused p^+-layer with a sheet resistance of 54 Ω/sq. and a 25 µm thick Al-layer on top. The wafers are diced in samples of 2×2 cm² and laser bonded with the passivated surface to a substrate with Al-foil using various pitches of 250 to 2000 µm at a constant line width of 83 µm.

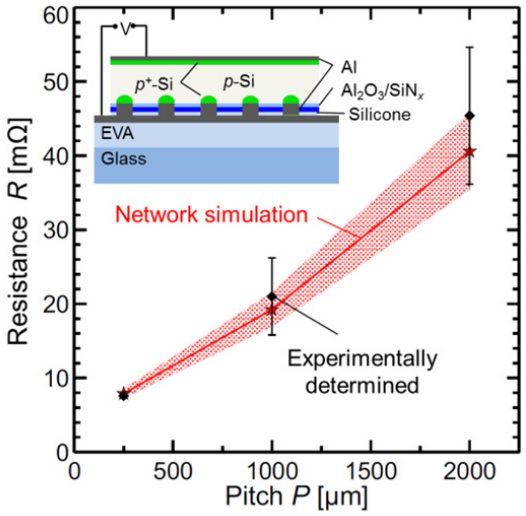

Fig. 3. Resistance *R* measured by 4-point-probe and values simulated by Spice network simulations in dependence on the pitch *P*. For both the uncertainty is given. The inset shows a cross-section of the sample used for determination of the contact resistance of the LFBC contacts.

Fig. 3 shows the resistance of the samples determined with 4-point-probe measurements. In order to determine the area related contact resistance of the LFBCs we perform network simulations based on LT-Spice, which include the impact of the lateral currents in the Al foil, the resistance of the Si bulk and of the emitter, the emitter-metal contact on the front side, and the contact resistance by the LFBCs, for details see [6]. Using the contact resistance of the LFBC as the only free variable in a fit of the simulation the experimental resistances [7] results in 3.52±0.74 mΩcm² per contact area.

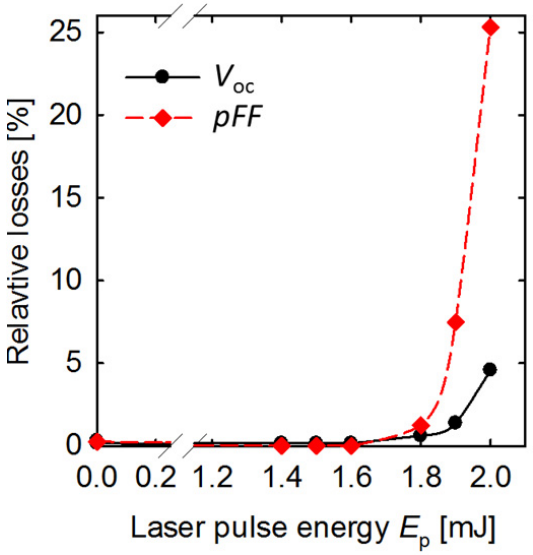

Fig. 4. Relative losses of open-circuit voltage V_{oc} and pseudo fill factor (*pFF*)before and after laser welding of Al foil to the Ag screen-printed busbar as determined by qssV_{oc}..

3.3. Front contact recombination

Laser-induced damage on the front side would result in a decrease of the open-circuit voltage V_{oc} and of the fill factor FF due to shunting. In order to detect the impact of the laser welding on the front, we measure the Suns-V_{oc} curve of PERC solar cells before and after laser welding using the "quasi-steady state open-circuit voltage method" (qssV_{oc}) [12] by a Suns-Voc-150 (Sinton Consulting inc.).

Fig. 4 shows the relative losses of the V_{oc} and the pseudo fill factor (*pFF*). For laser pulse energies E_p larger than 1.6 mJ we observe a significant decrease of the V_{oc} and *pFF* indicating shunting and laser induced damage at the cell's front side. For E_p smaller than 1.6 mJ no laser damage can be detected. Additionally to a damage-free interconnection the welding needs to stable during the module lifetime. We observe, that laser interconnections formed with a pulse energy of 1.1 mJ are stable under artificial aging, whereas modules without laser welding on the front side show a fast degradation of the *FF* in the first 10 or 20 cycles.

3.4. Proof-of-concept module

We process the solar cells on *p*-type wafer (ρ=2.3 Ωcm; 15.6 × 15.6 cm²; A = 240 cm²), which feature a textured front side with a 100 Ω/sq. emitter passivated by SiN_x. The front side is contacted by using Ag printing with a five busbar design. The rear side is passivated by a stack of AlO_x (5 nm) and SiN_x (200 nm). After firing the cells at a peak temperature of 850°C we laser dice them in five pieces of 15.6 × 3.08 cm² in size. We dice the solar cells next to the busbars, therefore the current path in the fingers to the next busbar is twice as long as in case of the reference cells. Two cell stripes are placed with the silicone coated rear side on the Al foil/EVA/glass stack. We fix the cells by a tape and laminate the module with an EVA layer and a glass on the front side. For laser processing we use a pulse energy E_p = 1.2 mJ for the rear and E_p = 1.35 mJ front side. The pitch for the line contacts on the rear side is 1500 µm. For the external connection we laser weld Al-clad Cu conductors to the Al foil, see Fig. 5.

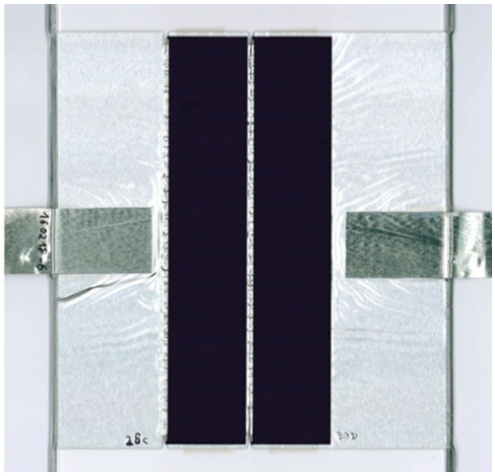

Fig. 5 Photograph of a module consisting of two cell stripes metallized and interconnected by an Al foil after final lamination with a front glass.

Table I gives the *I*-*V*-parameters of a reference cell with screen printed rear side contacts and of the two-cell module after laser processing on the front and the rear side. We measure the module without a shadow mask, so the short-circuit current density of the module, which is as high as of the reference PERC solar cells, can be affected by multiple reflections within the module. The module has a reasonable open circuit voltage per cell of 1293 mV/2=647 mV. The cells with Al screen-printed rear side, which are processed equally, show a V_{oc} of 652 mV

on a cell tester. The fill factor of 71.6% needs to be improved; it suffers from the series resistance caused by the fingers, in which the average transport path is two times longer compared to that of the initial cells, since we cut the cells next to the busbar. Additional series resistance contributions are caused by the transport in the Al foil between the cells and the distance of the cells to the external contacts. These additional series resistance losses account for a reduction in fill factor of 1.8% absolute.

Table I. *I-V*-parameters for the proof-of-principle module consisting of two 15.6 × 3.08 cm²-sized cells and the average values of four reference cells produced with the same process. The reference cells feature a screen printed rear side metallization in contrast to the interconnected cells. The module efficiency and short-circuit current density are related to the cell area. Characterization of the individual cells before interconnection is not possible, because the rear contact is formed only during module interconnection.

	A [cm²]	η [%]	FF [%]	V_{oc} [mV]	V_{oc}/cell [mV]	I_{sc} [A]	J_{sc}/cell [mA/cm²]
Reference cells	240	19.8	76.8	652	652	9.48	39.5
Module	96.1	18.4	71.6	1293	647	1.91	39.7

However, testing of the cells before interconnection is not possible due to the absence of the rear contact. Their thermal behavior during the firing step differs from the one of the reference cells with screen-printed rear side due to the latent heat of Al during melting. Therefore, the firing temperature might not have been optimal, which has an impact on the V_{oc} and FF.

Fig. 6 shows the relative changes of the *I-V*-parameters of a module interconnected by the presented laser processes depending on the number of humidity-free cycles. The module shows no degradation (< 1% in efficiency) in accelerated aging after 100 humidity-freeze cycles, which exceeds the required 10 humidity-freeze cycles according to the IEC norm 61215.

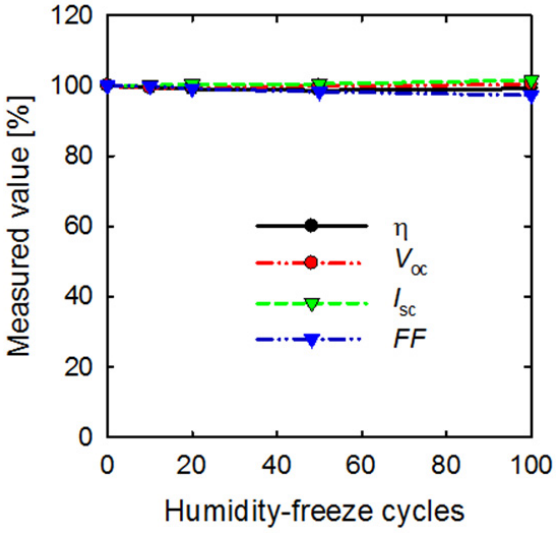

Fig. 6 Relative module *I-V*-parameters compared to initial values in dependence on the number of humidity-freeze cycles.

Fig. 6 shows the relative changes of the *I-V*-parameters of an module interconnected by the presented laser processes in the dependence on the number of humidity-free cycles. The module shows no degradation (< 1% in efficiency) in accelerated aging after 100 humidity-free cycles, which exceeds the required 10 humidity-free cycles according to the IEC norm 61215.

4. Conclusion

We demonstrated a process for simultaneous rear side metallization and interconnection of PERC solar cells. The laser bonded fired contacts result in surface recombination velocity for the laser contacted regions of 1000^{+1000}_{-500}cm/s, this is well below the recombination rates for LFC contacts (S_{cont} = 8600 cm/s 13). The contact resistance to *p*-type 0.5 Ωcm silicon is determined to be 3.52±0.74 mΩcm², which is as low as the contact resistivity of screen-printed Al contacts formed by laser contact opening and firing [14]. For the front side we use laser welding, where no laser damage is detected. The process presented here differs compared to the LFC process in that the Al foil is also used for cell interconnection. A second difference is the sealing of the space between the Al foil and the Si by using silicone. This eliminates the risk of the accumulation of water during accelerated aging, which has the potential to degrade the Al contacts [15]. A third difference is that we attach the Al foil to an EVA foil. The substrate confines the energy in the system [16], since the heated aluminium cannot escape in the opposite direction of the solar cells, and the LFBC process leads the formation of a thick BSF [6], which requires a high thermal budget. This explains the reduced surface recombination rates for the contacts compared to conventional LFC.

The proof-of-concept module reaches an efficiency of 18.4%. The efficiency is limited by the fill factor of the module and the initial cell performance. The cell process thus needs to be optimised for the presented interconnection scheme, e.g. the firing profile for a process without screen printed rear side metallization has to be adapted and the screen-printing for an elongated current path in the fingers has to be modified. A module interconnected with this processes is stable under 100 humidity-freeze cycles.

The LFBC and laser welding interconnection uses a thin (13 µm) Al foil that is as wide as the solar cells, instead of thick narrow solder-coated Cu ribbon (e.g. 0.2 ×1.5 mm²). Using a thin foil reduces the mechanical stress at the wafer edges, where the ribbon is led from the front side to the rear side [17]. Additionally, the thermo-mechanical stress induced after cool-down in the conventional soldering process is omitted. Since the Al metallization and the cell rear side are separated by a silicone layer, the parasitic absorption in the Al is reduced [7] resulting in an increase of the current. The newly introduced in-laminate laser welding of the Ag front side metallization offers also the possibility to contact solar cells that are highly sensitive to thermal processes, since the laser induced heat is small and high confined in the metal layers. The process can only be applied to stripes of solar cells due to the absence of busbars and ribbons, since the whole current transport on the cells front side is supported only by the fingers. Nevertheless, using cell stripes instead of full-sized cells reduces resistive losses [18] and is currently implemented for high power modules based on the shingle interconnection technique [19,20].

Acknowledgement

The authors thank Ulrike Sonntag and Sarah Spätlich for cell processing and Thomas Friedrich for sample preparation. This work was supported by the Federal Ministry for Environment, Nature Conservation, and Nuclear Safety under the contract FKZ 0325192 (CrystalLine) and by the State of Lower Saxony.

References

[1] Trina press release, 16th Dec. 2015, http://ir.trinasolar.com/phoenix.zhtml?c=206405&p=irol-newsArticle&ID=2122938.

[2] Engelhart P, Hermann S, Neubert T, Plagwitz H, Grischke R, Meyer R, Klug U, Schoonderbeek A, Stute U, Brendel R. Laser ablation of SiO2 for locally contacted Si solar cells with ultra-short pulses. Prog. Photovolt: Res. Appl. 2007;15(6):521–527.

[3] Schneiderlöchner E, Preu R, Lüdemann R, Glunz SW. Laser-fired rear contacts for crystalline silicon solar cells. Prog. Photovolt: Res. Appl. 2002;10(1):29–34.

[4] Nekarda J, Hörteis M, Lottspeich F, Wolf A, Preu R. Comparison of three different metallization concepts for LFC cells. In: Proceedings of the 25th European Photovoltaic Solar Energy Conference and Exhibition. 2010. p. 2245–2249.

[5] Bitnar BD, Fülle A, Heemeier MD, Krause AD, Kutzer M, Neuhaus HD, Schlegel K, Schneiderlöchner E, Weber T. Verfahren zur Herstellung eines Halbleiter-Bauelements A process for producing a semiconductor device(de 10 2006 044 936 B4): Google Patents; 2011. Available from: http://www.google.com/patents/DE102009010816B4?cl=en.

[6] Petermann JH, Schulte-Huxel H, Steckenreiter V, Kajari-Schroder S, Brendel R. Principle of Module-Level Processing Demonstrated at Single {a-Si:H/c-Si} Heterojunction Solar Cells. IEEE J. Photovoltaics 2014;4(4):1018–1024.
[7] Petermann JH. {Prozessentwicklung & Verlustanalysen für dünne monokristalline Siliziumsolarzellen und deren Prozessierung auf Modullevel}. Dissertation. Leibniz Universität Hannover, Hannover; 2014.
[8] Hannebauer H, Dullweber T, Baumann U, Falcon T, Brendel R. 21.2%-efficient fineline-printed PERC solar cell with 5 busbar front grid. Phys. Status Solidi RRL 2014;8(8):675–679.
[9] Ramspeck K, Bothe K, Schmidt J, Brendel R. Combined dynamic and steady-state infrared camera based carrier lifetime imaging of silicon wafers. J. Appl. Phys. 2009;106(11):114506.
[10] Kerr MJ, Cuevas A. General parameterization of Auger recombination in crystalline silicon. J. Appl. Phys. 2002;91(4):2473.
[11] Fischer B. Loss Analysis of Crystalline Silicon Solar Cells Using Photoconductance and Quantum Efficiency Measurements. Universität Konstanz, Konstanz; 2003.
[12] Sinton RA, Cuevas A. A Quasi-Steady-State Open-Circuit Voltage Method for Solar Cell Characterization. In: Proceedings of the 16th European Photovoltaic Solar Energy Conference and Exhibition. 2000. p. 1152–1155.
[13] Brendle W, Nguyen VX, Grohe A, Schneiderlöchner E, Rau U, Palfinger G, Werner JH. 20.5% efficient silicon solar cell with a low temperature rear side process using laser-fired contacts. Prog. Photovolt: Res. Appl. 2006;14(7):653–662.
[14] Kranz C, Lim B, Baumann U, Dullweber T. Determination of the Contact Resistivity of Screen-printed Al Contacts Formed by Laser Contact Opening. Energy Procedia 2015;67:64–69.
[15] Schulte-Huxel H, Blankemeyer S, Bock R, Merkle A, Kajari-Schröder S, Brendel R. Aging behaviour of laser welded {Al-}interconnections in crystalline silicon modules. Solar Energy Materials and Solar Cells 2012;106:22–26.
[16] Schulte-Huxel H, Kajari-Schroder S, Brendel R. Analysis of Thermal Processes Driving Laser Welding of Aluminum Deposited on Glass Substrates for Module Interconnection of Silicon Solar Cells. IEEE J. Photovoltaics 2015;5(6):1606–1612.
[17] Lamers MWPE, Tjengdrawira C, Koppes M, Bennett IJ, Bende EE, Visser TP, Kossen E, Brockholz B, Mewe AA, Romijn IG, Sauar E, Carnel L, Julsrud S, Naas T, Jong PC de, Weeber AW. 17.9% Metal-wrap-through {mc-Si} cells resulting in module efficiency of 17.0%. Prog. Photovolt: Res. Appl. 2012;20(1):62–73.
[18] Witteck R, Hinken D, Schulte-Huxel H, Vogt MR, Muller J, Blankemeyer S, Kontges M, Bothe K, Brendel R. Optimized Interconnection of Passivated Emitter and Rear Cells by Experimentally Verified Modeling. IEEE J. Photovoltaics 2016;published online:1–8.
[19] Schmidt W, Rasch K. New interconnection technology for enhanced module efficiency. IEEE Trans. Electron Devices 1990;37(2):355–357.
[20] Zhao J, Wang A, Abbaspour-Sani E, Yun F, Green MA, King DL. 22.3% efficient silicon solar cell module. In: Proceedings of the 25th IEEE Photovoltaic Specialist Conference. 1996. p. 1203–1206.